Differential movements and stresses in high-rise masonry veneers: Analysis

G. A. FENTON AND G. T. SUTER
Department of Civil Engineering, Carleton University, Ottawa, Ont., Canada K1S 5B6

Received September 17, 1985
Revised manuscript accepted July 4, 1986

In recent years a growing number of masonry veneer distress cases have occurred on high-rise structures. These cases are now known to be caused by the omission of a differential movement joint between veneer and structure. This paper reviews how these distress problems have arisen in a historical context and then presents the various movement parameters and relationships that must be considered. A computer model was developed to predict differential movements and resultant stresses when inadequate movement joints are provided. The paper gives an overview of the model and describes its capabilities. The application of the model to a case study structure is treated in a subsequent paper.

Au cours des dernières années, un nombre sans cesse croissant de cas de désordres des placages de maçonnerie se sont produits dans les constructions en hauteur. Nous savons maintenant que ces désordres sont causés par l'absence d'un joint de mouvement différentiel entre le placage et la structure. Cette communication examine d'un point de vue historique comment ces problèmes sont apparus et présente ensuite les divers paramètres de mouvement et les diverses relations dont il faut tenir compte. Un modèle informatique a été mis au point afin de prédire les mouvements différentiels et les contraintes qui en résultent lorsque des joints de mouvement inadéquats sont exécutés. Cette communication fournit une description du modèle et de ses possibilités. L'application du modèle à une étude de cas sera traitée dans une communication subséquente.
[Traduit par la revue]

Can. J. Civ. Eng. **13**, 700–712 (1986)

1. Introduction

Over the past decade an increasing number of masonry veneer problems have come to plague designers and owners. Such problems generally have been caused by the failure to consider differential movements between masonry veneer and structure. The most common veneer support detail consists of a steel shelf angle attached to the structure at each floor level as shown in Fig. 1. We know today that the provision of an adequate movement joint or soft joint under each shelf angle will ensure that the masonry veneer movements will occur independently of the structure. In the absence of a soft joint, veneer distress typically consists of spalling, crushing, cracking, bulging, and buckling. Figures 2–4 illustrate some of these distress conditions.

Why have these differential movement problems surfaced, particularly in the last decade? The reasons are complex and pertain partly to:

— Incomplete knowledge about material deformations: concerning reinforced concrete, reasonably accurate prediction of shrinkage and creep movements of columns only became possible in the early to mid-1970's; concerning the deformation of clay brick masonry, moisture expansion, freezing expansion, and shelf angle corrosion expansion were only recognized by the design profession in the late 1970's and even today are not well understood.

— Progressive changes in building codes: concerning reinforced concrete, higher service load stresses led to taller structures whose columns undergo greater elastic and creep movements; concerning clay brick masonry, modern engineered masonry design allowed more slender elements and required high-strength cement mortars, which are less forgiving than the traditional softer lime mortars.

— Lack of masonry education: a large step forward in Canadian masonry design occurred in 1965 when for the first time the masonry code allowed design by an engineered rather than the traditional rule-of-thumb approach. This step was not accompanied by the appropriate educational programs in industry, universities, and technical colleges. For instance, it was only in the mid to late 1970's that universities introduced masonry into their graduate programs, and even today few undergraduate engineering students are exposed to masonry design. The First Canadian Masonry Symposium was held in 1976 and it was in fact at this event that the first comprehensive paper dealing with veneer differential movement problems was presented (Suter and Hall 1976).

— The existence of a grey area of responsibility between design professionals: traditionally, the architectural profession has been responsible for the detailing of a structure's cladding. Increasing sophistication of modern building enclosures — and the shelf angle detail is only one of many aspects — requires input from structural engineers and building scientists. The lines of responsibility in this complex situation are often not clearly defined and in cases of building enclosure distress it is left up to courts of law to assign responsibility.

— Inadequate fees: in many instances low professional fees do not permit a proper level of supervision and inspection by qualified personnel during construction. Even when the shelf angle detail is properly designed, poor or unknowledgable workmanship can easily lead to hard joints where soft joints are specified.

To ensure that differential movements between masonry veneer and structure are properly designed for, the types and magnitudes of material deformations need to be known. This paper looks in detail at the deformational properties of the most common building materials — clay brick, concrete block, concrete, and steel — and presents a method of predicting differential movements and resulting stresses when these materials are used in high-rise structures (Fenton 1984; Fenton and Suter 1985). The deformation relationships given in the paper are programmable in today's microcomputers, allowing the designer to arrive at required soft joint widths or to investigate stress levels in distressed veneers. The long-term material deformations considered are those arising from creep, moisture migration, and corrosion expansion whereas the short-term re-

NOTE: Written discussion of this paper is welcomed and will be received by the Editor until March 31, 1987 (address inside front cover).

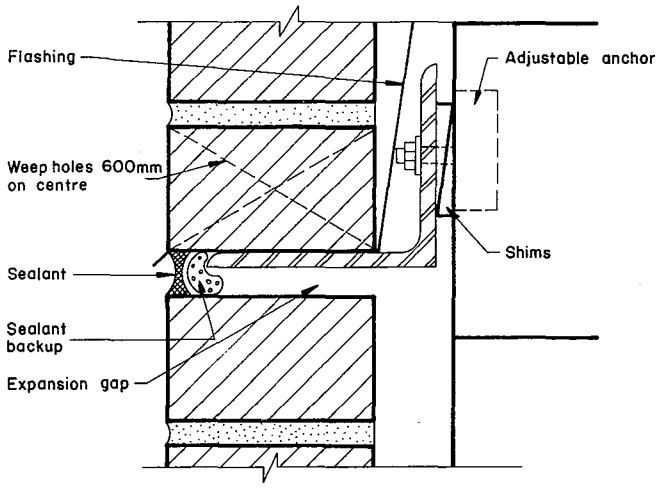

FIG. 1. Shelf angle detail showing proper movement joint.

versible or partially reversible deformations considered arise from elastic, thermal, and freezing expansion effects.

To predict the magnitude of differential movement at the outer skin of a high-rise structure, a computer program was developed. The program first calculates the absolute unrestrained movement in each material at a specified time, then compares these movements, and finally arrives at the restrained differential movement and corresponding stresses.

Such a model can be used to evaluate and optimize the design of a veneer system. In this journal issue, the accompanying paper entitled "Differential movements and stresses in high-rise masonry veneers: Case study" looks at factors that typically lead to distress of the veneer on a reinforced concrete structure. Design recommendations are made along with a discussion of workmanship details.

The computer program is able to model load-bearing masonry structures as well as reinforced concrete and steel structures. This paper will concentrate on reinforced concrete structures clad with a clay brick masonry veneer since maximum differential movements and most problems in practice occur for such a combination.

2. Unrestrained deformations

2.1 General

Table 1 shows the types of deformations considered for each of the vertically spanning structural materials that might be found at the perimeter of a building. In this section relationships predicting the magnitude of these linear deformations will be presented with a view towards their use in a computer program.

2.2 Elastic

2.2.1 Concrete

The modulus of elasticity of concrete has been related to a number of parameters, the most common being density and compressive strength. The Canadian code CAN3-A23.3-M84 (CSA 1984*a*) gives the modulus of elasticity of concrete as

$$[1] \quad E_c = 0.043\gamma_c^{1.5}\sqrt{f'_c} \text{ (MPa)}$$
$$\simeq 5000\sqrt{f'_c} \qquad \text{for normal density concrete}$$

Based upon European experience, the Comité Européen du Béton (CEB) found the mean modulus of elasticity of normal weight concrete at 28 days to be somewhat higher than suggested by [1] (CEB 1976):

$$[2] \quad E_c(28) = 11\,875\sqrt[3]{f'_{cm}(28)} \text{ (MPa)}$$

In lieu of a specified 28-day elastic modulus, the program defaults to the use of [2]. The CEB also found the elastic modulus to vary with time, becoming stiffer with age:

$$[3] \quad E_c(t_i) = E_c(28)\sqrt[3]{\frac{f'_{cm}(t_i)}{f'_{cm}(28)}}$$
$$= E_c(28)\left[0.3103 \ln (1.1631t_i) - 0.3073 \ln\left(1 + \frac{t_i}{93.09}\right)\right]^{1/3}$$

Equation [3] is used to predict the elastic modulus of the concrete at any time in the building's life.

2.2.2 Concrete block masonry

Concrete block masonry is a composite material whose elastic properties are dependent on the individual properties of the block unit, mortar, and grout if present. Sturgeon *et al.* (1980) developed a relationship between the masonry compressive strength f'_m, based on net area, and the elastic modulus of ungrouted concrete block masonry:

$$[4] \quad E_{ug} = 432f'_m + 4668 \text{ (MPa)}$$

In turn, Eskenazi *et al.* (1975) present a relationship between masonry strength and the individual block and mortar strengths:

$$[5] \quad f'_m = 0.644f'_{bl} + 1.184\sqrt{f'_{mort}} - 3.405 \text{ (MPa)}$$

Typically, the elastic moduli of grouted prisms are substantially less than those of hollow prisms, even for grout stengths in excess of the block unit strengths. For fully or partially grouted block-work walls, Sturgeon *et al.* (1980) propose the following relationship for the calculation of the elastic moduli:

$$[6] \quad E_{bl} = \frac{0.56E_{gr}(\alpha)(1 - \psi) + E_{ug}(\psi)}{(\alpha)(1 - \psi) + \psi}$$

where E_{ug} is determined from tests or according to [4] and E_{gr} is found from [1] or [2]. Other options are available to the program user to calculate E_{bl}, however, [4] and [6] are the default.

Although little research is available on the variation of the elastic modulus of concrete block masonry with time, the use of [3] with E_{bl} in place of E_c shows reasonable agreement with limited NCMA (1977) test data, particularly for grouted prisms, and has been used for this purpose in the program.

TABLE 1. Sources of material deformation

Type of deformation	Material			
	Steel	Reinforced concrete	Concrete block	Clay brick
Elastic	x	x	x	x
Thermal	x	x	x	x
Shrinkage		x	x	
Creep		x	x	x
Moisture expansion				x
Freezing expansion				x
Corrosion expansion				x

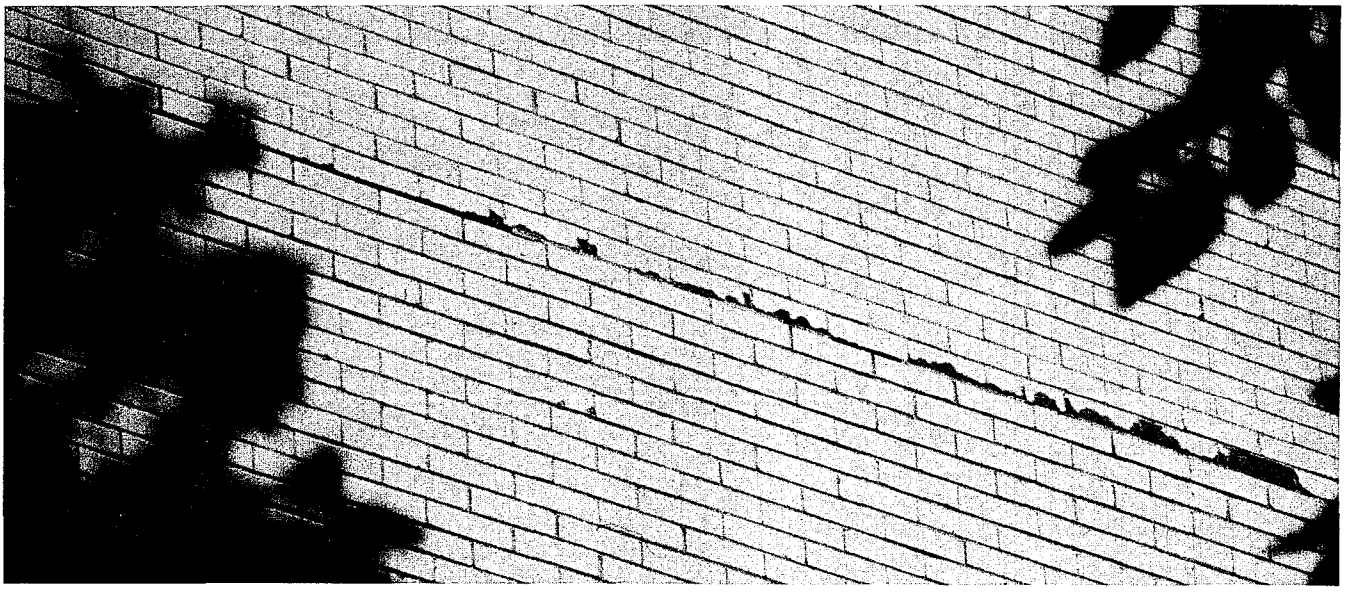

FIG. 2. Spalling of masonry veneer at a steel shelf angle location.

FIG. 3. Removal of a section of the masonry veneer shows cracking and crushing of the brick under the shelf angle.

2.2.3 Clay brick masonry

As with concrete block masonry, clay brick masonry is also a composite material with elastic properties dependent on both brick and mortar. Many empirical relationships have been suggested by various researchers over the years in which the elastic modulus is related to the compressive strength of either the brick unit or the masonry as a whole. The Canadian masonry code CAN3-S304-M84 (CSA 1984*b*) gives

$$[7] \quad E_m = 1000 f'_m \text{ (MPa)} \leq 20\,000$$

which tends to yield moduli somewhat higher than predicted by either Eskenazi *et al.* (1975):

$$[8] \quad E_m(28) = 220.6 f'_{br} + 1000 \text{ (MPa)}$$

or Grimm (1981):

$$[9] \quad E_m(28) = 7957[\ln (f'_m) - 1.12] \text{ (MPa)}$$

If an elastic modulus is not specified by the program user, either [8] or [9] is used, depending on the material properties known. Grimm further provides a relationship giving variation of elastic modulus with time:

$$[10] \quad E_m(t_i) = E_m(28) + 7957[\ln \{31 + \ln (t_i)\} - 3.536] \text{ (MPa)}$$

Note that the elastic modulus varies with the double logarithm of time and so grows very slowly—about 6% in 5 years. Over the same interval, CEB (1976) expects the elastic modulus of concrete to increase by about 13%. Because of the nature of brick masonry, with most of the hardening taking place in the mortar joint, [10] appears to be reasonable and has been used in the program.

2.2.4 Steel

The elastic modulus of steel is assumed throughout to be 200 000 MPa.

2.3 Thermal

The thermal strain in each of the building elements is determined from

$$[11] \quad \epsilon_{th} = \alpha_{th}(T_i - T_p)$$

where T_p is the temperature of the element at the time of its placement and is assumed to be equal to the mean ambient air temperature with a lower bound of −5°C, since heating is generally provided during winter construction months. The determination of the element temperatures, T_i, at the time of interest is carried out in two ways:

TABLE 2. Coefficients for use in the calculation of the shrinkage function $\beta_s(t)$ according to [15]

d_m	h	j	k	m	n	r	P	Q
50	0.19464	0.56397	0.88267	5.1596	0.13073	283.108	1.70	1.45
100	0.18801	0.27226	0.08482	7.6606	0.10532	662.446	1.75	1.70
200	0.21292	0.06315	0.17134	22.8553	0.06661	1355.882	1.10	2.80
400	0.24861	0.01726	0.14650	98.8952	0.08884	2822.085	1.50	2.60
800	0.36080	0.00312	0.18806	468.9953	0.10275	4683.308	1.80	3.30
1600	0.36503	0.00150	0.16160	793.5471	0.11509	9451.367	2.20	3.00

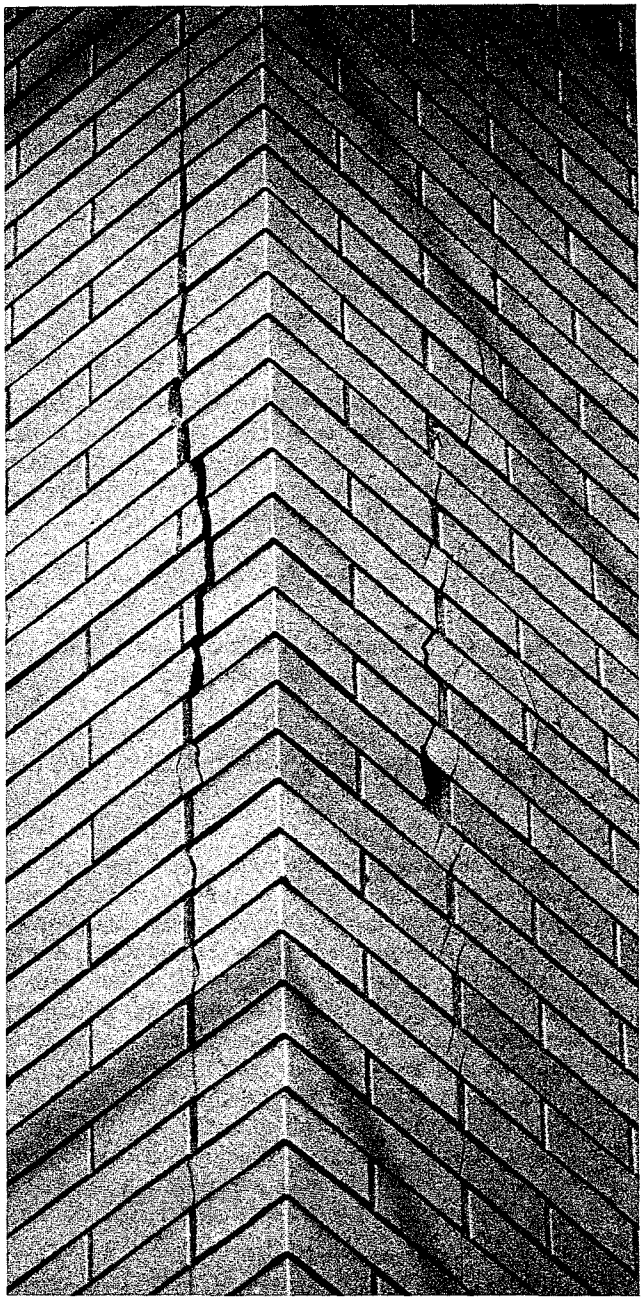

FIG. 4. Vertical corner cracking of masonry veneer associated with lack of movement joint and discontinuous shelf angle at corner.

(1) For average temperatures, which contribute to creep stresses, and for the minimum winter temperatures, a one-dimensional steady-state heat flow analysis is applied to the exterior wall sandwich. The wall sandwich is composed of up to eight layers including the air cavity. The thickness, density, thermal conductivity, specific heat, emissivity, and absorptivity of each layer are specified by the program user or calculated internally depending on material type.
(2) For extreme summer conditions, a one-dimensional transient heat flow analysis is performed on the exterior wall sandwich over a 24 h period. The transient analysis allows the effect of solar radiation on the veneer and interior layers to be included. The program automatically selects the temperature set with the greatest temperature differential between the veneer and structure — due to thermal mass and phase lag, this will not necessarily coincide with the maximum veneer temperature.
Typical coefficients of thermal expansion for concrete and masonry can be found in Appendix B. The coefficient of thermal expansion of steel is about 12 μm/(m·°C).

2.4 Moisture

2.4.1 Concrete

The gradual moisture loss from concrete results in a slight volume change, referred to as shrinkage. The amount of shrinkage an element will experience depends on the concrete age, the relative humidity and temperature of the environment, the volume-to-surface ratio, and the concrete composition. The relationship predicting concrete shrinkage suggested by Grimm (1981), tends to be somewhat complex, requiring the knowledge of such factors as the calcium chloride content of the concrete. A somewhat simpler relationship is suggested by CEB (1980) to be

$$[12] \quad \epsilon_{sh}(t_i, t_0) = S_1 S_2 [\beta_s(t_i) - \beta_s(t_0)]$$

with

$$[13] \quad S_1 = -7.721 \times 10^{-4}\left(1 - \frac{RH}{100}\right)^{0.7737}$$

$$[14] \quad S_2 = 0.6 + \sqrt{\frac{18}{d_m}}$$

$$[15] \quad \beta_s(t) = h \ln(jt) + k \ln\left[1 + \left(\frac{m}{t}\right)^P\right] - n \ln\left[1 + \left(\frac{t}{r}\right)^Q\right]$$

where d_m is the effective thickness of the concrete and is determined according to [C.6] in Appendix C. The coefficients h, j, k, m, n, P, Q, and r in [15] depend on the effective thickness d_m and are shown in Table 2. Although the CEB relationships tend to give shrinkage values somewhat lower than those predicted by Grimm, they were adopted for use in the computer program if a known ultimate shrinkage value is not specified.

To interpolate for intermediate values of d_m (for example, d_m = 275 mm), the following method is used:
(1) Let d_1 be the next lower value of effective thickness shown in Table 2 (i.e. for d_m = 275 mm, d_1 = 200 mm) and d_2 be the next higher value (i.e., d_2 = 400 mm).
(2) Calculate $\beta_{s1}(t)$ for the effective thickness d_1 and $\beta_{s2}(t)$ for d_2.

TABLE 3. Typical values of ultimate shrinkage of mortar (from Sturgeon 1978)

Ratio of cement:lime:sand	Ultimate unrestrained shrinkage (%)
1:0:3	0.037
1:0:6	0.028
1:0:8	0.031
1:1:6	0.035
1:2:9	0.027
1:3:12	0.017

(3) Calculate an interpolation factor η as follows:

$$[16] \quad \eta = [1.2 - 0.0869 \ln (t)]\left[\frac{d_m - d_1}{d_2 - d_1}\right]^{15d_m^{-0.7}}$$

(4) Calculate $\beta_s(t)$ as follows:

$$[17] \quad \beta_s(t) = \beta_{s1}(t) - \eta[\beta_{s1}(t) - \beta_{s2}(t)]$$

2.4.2 Concrete block masonry

The unrestrained shrinkage of concrete block masonry in the vertical direction is found as a weighted function of the individual grout and shell shrinkages:

$$[18] \quad \epsilon_{sh}(t_i) = \left[\frac{\alpha(1 - \psi)}{\alpha(1 - \psi) + \psi}\right]\epsilon_{shgr}(t_i) + R_{bl}\left[\frac{\psi}{\alpha(1 - \psi) + \psi}\right]\epsilon_{shbl}(t_i, t_0) + (1 - R_{bl})\left[\frac{\psi}{\alpha(1 - \psi) + \psi}\right]\epsilon_{shmo}(t_i)$$

The shrinkage strain of the grout, $\epsilon_{shgr}(t_i)$, from its time of placement is derived from [12] as

$$[19] \quad \epsilon_{shgr}(t_i) = -7.721 \times 10^{-4}\left(1 - \frac{RH}{100}\right)^{0.7737} \times \left[0.6 + \sqrt{\frac{18}{d_m}}\right]\beta_s(t_i)$$

where d_m is calculated from [C.7] in Appendix C, and $\beta_s(t_i)$ is determined according to [15].

The shrinkage of mortar is proposed by Grimm (1981) to be

$$[20] \quad \epsilon_{shmo}(t_i) = \epsilon_{msu}[1 - 2.35 \times 10^{-7}(RH)^{3.3}] \times \left[\frac{t_i}{t_i + 26e^{0.0142D_m}}\right]$$

with typical values of the ultimate mortar shrinkage strain, ϵ_{msu}, given in Table 3.

The shrinkage strain relationship given in [12] for concrete was also found to have excellent agreement with NCMA (1961) test data on concrete blocks. HHFA (1954) found that the rewetting of concrete blocks resulted in an expansion of about one-quarter the shrinkage that had already occurred. Since the addition of grout adds a considerable amount of moisture to the block, [12] was modified as follows to predict the shrinkage strain of grouted concrete block:

$$[21] \quad \epsilon_{shbl}(t_i, t_0) = \epsilon_{blsu}[\beta_s(t_i) - (1 - 0.25\alpha)\beta_s(t_0)]$$

The amount of moisture expansion due to wetting is taken into account through the term $(1 - 0.25\alpha)$, where the assumption is that the degree of wetting is directly proportional to the fraction of cores grouted. If the block is wetted before laying, the term $(1 - 0.25\alpha)$ becomes equal to 0.75 (Fenton 1984).

If the ultimate shrinkage strain of the block unit is unknown, it is calculated from

$$[22] \quad \epsilon_{blsu} = S_1 \cdot S_2$$

using [13] and [14].

2.4.3 Clay brick masonry

The response to the environment of clay brick after it has been fired is radically different from that of concrete block. Palmer (1931) was one of the first to experimentally verify that clay brick gradually expands with exposure to the atmosphere, whereas concrete usually shrinks. Although it is generally agreed that the moisture expansion of clay varies with the logarithm of time, its ultimate magnitude is highly variable—dependent not only on the composition of the clay but also on firing temperature and environmental conditions. The computer program makes use of the following relationship derived from work by Grimm (1981):

$$[23] \quad \epsilon_{bm}(t_i) = \epsilon_{bmt}\left[\frac{3.12\{\log_{10}(t_i + 2.3) - \log_{10}(t_0 + 2.3)\}}{3.12 \log_{10}(t_t + 2.3) - 1}\right] \quad (t \text{ in months})$$

Equation [23] depends on either a delayed moisture expansion test, as described by Grimm, or an estimated moisture expansion value for ϵ_{bmt}. If ϵ_{bmt} is the measured moisture expansion strain from a 4-h accelerated steam test, the program makes use of McDowall and Birtwistle's (1970) relationship

$$[24] \quad \epsilon_{bm}(t_i) = 0.6013\epsilon_{bmt}[\ln (t_i + 2.298) - \ln (t_0 + 2.298)] \quad (t \text{ in months})$$

To calculate the net expansion of the brick masonry, the program includes the effect of mortar shrinkage, i.e.,

$$[25] \quad \epsilon_m(t_i) = R_{br}\epsilon_{bm}(t_i) + (1 - R_{br})\epsilon_{shmo}(t_i)$$

where the shrinkage strain of the mortar, ϵ_{shmo}, is determined from [20].

2.5 Creep

The creep of concrete, concrete block, and clay brick masonry has been found to be affected not only by the magnitude of the applied stress but also by the age of the material at the time of loading. Thus as the load or stress changes, the accurate calculation of creep must take an incremental form with an appropriate adjustment for the age at which the incremental stress was applied. In this section, incremental creep strain relationships will be presented for each material as they are implemented in the program. These relationships are based on the principle of superposition, which states that creep deformations due to stress increments applied at different intervals of time are additive. The principle of superposition is generally agreed to hold true within the range of service load stresses.

2.5.1 Concrete and concrete block

Of the methods proposed to predict the creep strain due to incremental loading in concrete, the best was found to be that put forward by CEB (1980). Both Fintel and Khan (1969) and Grimm (1981) present simplified methods but both have the following disadvantages:

(1) The creep strain during the construction phase is difficult to determine.

(2) Since they rely on the final stress on the concrete column after completion of the building, the effects of transfer of load

to the block work or brick masonry cannot be considered—the magnitude of this transfer depends on the magnitude of the deformation in the column.

The creep strain in concrete at any instant in time due to a stepwise varying stress is proposed by CEB to be

$$[26] \quad \epsilon_{cr}(t_i) = \sum_{j=1}^{i-1} k_j(\sigma_j - \sigma_{j-1}) \cdot \Phi(t_i, t_j)$$

The creep function, $\Phi(t_i, t_j)$ giving the specific creep at the time of interest is quite complex and its derivation can be found in Appendix C.

Equation [26] was found to be in close agreement with NCMA (1977) creep test data on concrete block masonry when t_i' and t_j' were used in place of t_i and t_j, where

$$[27] \quad t_i' = t_i + t_{eff}$$

$$[28] \quad t_j' = t_j + t_{eff}$$

and t_{eff} is the effective age of the concrete block masonry at the time of construction. This effective age is dependent on the amount of grout introduced into the wall and is found from

$$[29] \quad \ln (t_{eff} + 1) = \ln (t_{bl} + 1)\left[\frac{0.44 - \alpha(1 - \psi)}{0.44}\right]$$

for a standard hollow block

2.5.2 Clay brick masonry

Although a fair amount of research has been performed on the relationship between creep and time for clay brick masonry, very little research has dealt with the effect of the age at loading. To the authors' knowledge, the most thorough investigation into the latter aspect was carried out by Poljakov (1962), who arrived at the relationship

$$[30] \quad \epsilon_{cr} = A_b\left(\frac{\sigma_i}{\sigma_{ult}}\right)(t_i - t_1)^{1/7} \cdot f_a$$

where f_a = age-at-loading correction factor

$$[31] \quad = 0.1 + 1.82e^{-0.3\sqrt[4]{t_1}}$$

Unfortunately Poljakov's relationship, [30], gives creep strains that are in relatively poor agreement with test observations by Warren and Lenczner (1981) and so was not used in the program. However, the age-at-loading correction factor of [31] does appear to be quite reasonable when compared with similar factors recommended by Grimm (1981) for clay brick masonry and CEB (1980) for concrete.

Lenczner (1970, 1980) and Warren and Lenczner (1981) have conducted an intensive study into the relationship between creep and time for clay brick walls loaded at 28 days. The following relationships have been derived from the work done by Warren and Lenczner (1981):

$$[32] \quad \epsilon_{cr} = \sigma_i \times 10^{-5}\left[\frac{t_i - 28}{a + b(t_i - 28)}\right]$$

where the constants a and b are determined from the brick unit strength f_{br}' and construction conditions as follows:

(1) For bricks laid dry.

$$[33] \quad b = \frac{5.171\sqrt{f_{br}'} - 19.158}{734.6 - 61.53\sqrt{f_{br}'}}$$

$$[34] \quad a = 3.8024 \ln (b) + 18.2096$$

Equations [33] and [34] are considered reliable for values of f_{br}' between 22 and 143 MPa.

(2) For bricks laid wet,

$$[35] \quad b = \frac{5.171\sqrt{f_{br}'} - 19.158}{325.4 - 30.58\sqrt{f_{br}'}}$$

$$[36] \quad a = 7.3876 \ln (b) + 21.7915$$

Equations [35] and [36] are considered reliable for values of f_{br}' between 29 and 113 MPa.

It is assumed that the difference between the wet and dry relationships reflects the effect of brick suction on the mortar properties. Since North American bricks in general have lower rates of suction than their British counterparts, it is believed that the 'wet' relationships more closely describe the North American brick masonry, even when bricks are laid dry.

Combining [32] with the age-at-loading correction factor of [31] gives the incremental creep strain relationship used in the program:

$$[37] \quad \epsilon_{cr}(t_i) = \sum_{j=1}^{i-1} k_j(\Delta\sigma_j \times 10^{-5})\left(\frac{(t_i - t_j)}{a + b(t_i - t_j)}\right) \times (0.1 + 1.82e^{-0.3\sqrt[4]{t_1}})$$

2.6 Freezing expansion of clay brick

When clay brick freezes, it usually undergoes a certain amount of expansion. Tests performed by Davison (1980) indicated a large variability in the magnitude of this expansion, either upon first freezing or in the permanent strain that exists after rethawing. Temporary freezing expansion strains of between 0.03 and 1.19 mm/m were observed with an average of 0.44 mm/m; permanent strains ranged from 0 to 0.56 mm/m with an average of 0.16 mm/m. It should be noted that in all cases the brick was saturated prior to freezing and so the freezing expansion of bricks on site would be expected to be somewhat lower. The computer program assumes that freezing expansion specified by the user only occurs if the mean ambient temperature drops below that required for freezing and if the bricks do not undergo freezing prior to construction, i.e. while stacked on site.

2.7 Corrosion expansion of steel shelf angles

The formation of corrosion products between the masonry and the supporting shelf angle will force the masonry to move upwards or, conversely, the shelf angle will be forced down. If the shelf angle is adequately protected by coatings, flashing, and weep holes, then the corrosion will be negligible. However, if unprotected steel is intermittently exposed to water, then corrosion will occur.

Grimm (1981) estimates the effective strain in the masonry due to corrosion expansion to be

$$[38] \quad \epsilon_{co} = (K_c - 1.0)\left(\frac{\Delta d_c}{h}\right)\left(\frac{t_i - t_{sp}}{t_{sa} - t_{sp}}\right)^{0.3}$$

Equation [38] depends on the measurement of the amount of corrosion that has occurred some time after the placement of the shelf angle. In many cases such a measurement is not feasible and the designer must estimate Δd_c based on past experience. Stetina (1965) estimates the average rate of unprotected steel surface corrosion to be about 0.13 mm/year when exposed to generous amounts of water and oxygen. This rate may drop to about 0.01 mm/year if the surface is left relatively dry after the first year.

3. Veneer–structure interaction

3.1 General

Once the unrestrained deformations occurring in each mate-

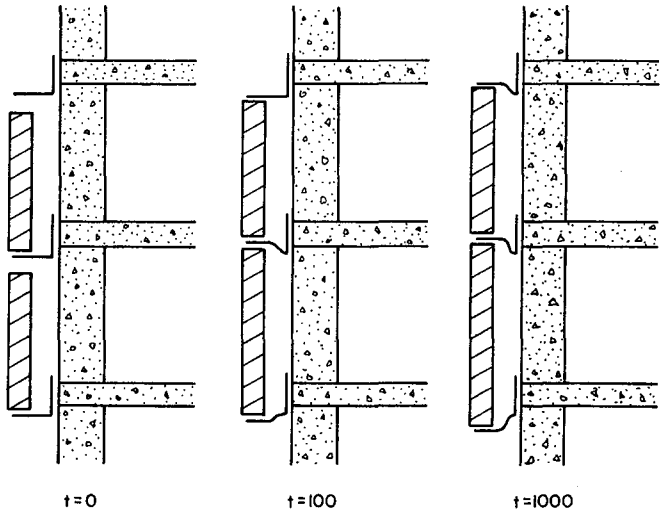

FIG. 5. Veneer–frame interaction model.

rial have been calculated in the computer program for the time of interest, they are summed to yield the net deformation in each vertically spanning element. If the element is reinforced, the calculation of its net deformation is slightly more complex in that the steel and concrete strains must be combined through compatibility and elastic equations assuming complete bonding between the two. The net deformations are then compared at each building level to determine if interaction takes place between the veneer and the structure and to what extent. Figure 5 illustrates the interaction between a growing clay brick veneer and a shortening structure as time goes on. In this case the veneer is assumed to be supported at regular intervals by steel shelf angles, as would be true on most steel and reinforced concrete structures. Load-bearing masonry structures, on the other hand, typically employ veneers that run continuously from foundation wall to roof and are tied back to the load-bearing masonry walls by means of metal ties at, for example, every second block course over the height of the building. For the purpose of this analysis, the ties are considered to act as if lumped at the slab level of every storey.

The deformation of the shelf angle results in a 'shear' force set up in the angle, which manifests itself as an axial force acting on the veneer in one direction, and on the structure in the other. The magnitude of the shear force depends on:
(1) the magnitude of the relative deformations between the structure and the veneer,
(2) the size of the movement joint left below the shelf angle,
(3) the stiffness and yield point of the shelf angle,
(4) the vertical stiffness of the veneer and the structure (both are assumed to be fully elastic over the range of stresses expected),
(5) the relative movements occurring in the levels above and below the level being considered.

Also shown in Fig. 5 is the effect one panel can have on another, i.e., the lower panel is forcing the upper panel upwards into contact with its overlying shelf angle. It can be seen that the stresses occurring in a veneer panel are not solely dependent on its deformation relative to the adjacent frame but also on relative movements occurring above and below it.

Such a system can be modelled either iteratively or through the use of a set of simultaneous equations. In the computer program the iterative solution was selected to accommodate many sources of nonlinearity, such as:
(1) yielding of the shelf angles,
(2) changing stiffness of the structure due to the slab lifting off the infill blockwork (this will occur if the cumulative shear forces in the shelf angles are sufficiently large),
(3) the inability of the shelf angles to exert an upwards force on the underlying brick panel (i.e. if the brick is not in contact with the upper shelf angle, no stress occurs in the panel).

In order to include the effects of creep on the veneer–structure interaction, the analysis must be broken up into a series of time intervals. Within each time interval the following steps are taken by the computer program as illustrated by the flow chart in Appendix D:
(1) Calculate the net structural deformation at each level.
(2) Calculate the net unrestrained brick veneer deformation at each level.
(3) Calculate the flexibility of the structure and veneer at each level.
(4) Calculate the 'at rest' position of the upper shelf angle at each level (including the deformation due to the forces transmitted through the veneer from above according to the previous iteration).
(5) Calculate the unrestrained position of the upper surface of the brick veneer panel at each level.
(6) If the positions calculated in steps (4) and (5) overlap, then calculate the deformed positions of both the upper and lower shelf angles and the resulting shelf angle shear forces at each level.
(7) Check to see if either (or both) the upper or lower shelf angle yields. If so, introduce the appropriate limiting force(s) and recalculate the deformed positions of both shelf angles, assuming plastic behaviour.
(8) Check to see if the structure flexibility changes due to lift-off from the block work. If so, calculate the new flexibility value and return to step (6).
(9) Repeat steps (4) to (8) until the shelf angle shear forces at each level remain approximately constant from one iteration to the next.
(10) Calculate the new stresses acting on each element at each level.

3.2 Computer program

The computer program was developed to study the interaction between a veneer and its supporting structure, particularly with regard to the stresses arising in each structural element as well as differential movements. Because of the program's size, it is not possible to include a listing in this paper. However, the program is available from G. T. Suter, Department of Civil Engineering, Carleton University, Ottawa, Ont., who should be contacted concerning the medium of transfer for this program. A flow chart of the iterative procedure described in the previous section is included in Appendix D. The program has the following capabilities and limitations:
— Reinforced concrete, structural steel, and load-bearing masonry structures can be modelled.
— Veneer can be connected to the frame by masonry ties alone, or by ties and shelf angles at single or multiple floor spacing and with various movement joint widths.
— Yield and stiffness properties of the ties and (or) shelf angles are considered in the analysis. Ties are assumed to act as if lumped at each floor level.
— Up to eight different 'times of interest' can be specified after construction is completed.
— The veneer must be present on at least one level of the

building and must be of clay brick.
—The maximum number of storeys, including basements, is 25.
—All forces are assumed to act concentrically and all materials, except ties and shelf angles, are assumed to be linearly elastic.

The shelf angle stiffness is defined here as the force required to deform the outer tip of the angle upwards one unit relative to the adjacent column. Thus the force exerted by the shelf angle on the underlying brick masonry is proportional to its tip deflection until yield is achieved. Beyond yield this force is assumed to remain constant.

The predicted stresses generated by the computer program are based on the assumption that all forces act concentrically and uniformly. In fact, it is known that this is rarely the case. Suter and Hall (1976) found that shelf angle forces are often applied to the inside edge of the masonry owing to rotation of the angle as it deforms. In addition, forces transmitted through the veneer from above are often channelled through a narrow mortar joint at the toe of the shelf angle. Local stresses can be many times greater than the predicted concentric stresses due to these stress concentration factors. Also, the eccentricity of the load could lead to buckling or cracking of the veneer, particularly if the masonry ties are omitted or poorly installed in the region of the slab.

The transfer of forces from the column to the slab and from the slab to the shelf angle is also assumed to be uniform, i.e., the slab is assumed to be infinitely stiff. In fact, the flexibility of the slab will lead to some additional stress concentration in the immediate region of the column in both the clay brick veneer and the concrete block infill.

Just what typical differential movements occur between veneer and structure and what typical stresses can be expected due to the omission of a soft joint at shelf angles is presented in a follow-up paper entitled "Differential movements and stresses in high-rise masonry veneers: Case Study."

4. Concluding remarks

For the differential movement problems of masonry veneered structures, the paper reviewed the causes of distress and presented a method of predicting such movements. Although, in the authors' oponion, the deformational relationships and analysis presented here allow most of the aspects affecting veneer stresses to be considered, the mathematical model is only as good as the data used. Many of the material properties are derived from controlled laboratory tests and its is difficult to know how closely these relate to onsite properties in a highly variable environment. Other aspects such as the *in situ* shelf angle stiffness can only be determined by careful testing on an actual structure. Also, thermal properties, such as emissivity and absorptivity, can only be ascertained from the materials to be used. In most cases this testing is not feasible and typical values and ranges must be relied upon. If reasonable values for deformation parameters are selected, the computer program results are seen to be in substantial agreement with distress observed on actual structures.

Acknowlegements

The financial support for this work by the Natural Sciences and Engineering Research Council of Canada and the Canadian Masonry Research Council is gratefully acknowledged.

ANDERSON, G. W. 1976. The design of brickwork for differential movement. Brick Development Research Institute, Australia, Techniques No. 6, 2nd series.

BAKER, M. C. 1964. Thermal and moisture deformations in building materials. Canadian Building Digest, CBD-56, 4 p.

BERGQUIST, L. 1979. Masonry veneer walls. Fifth International Brick Masonry Conference, Brick Institute of America, pp. 275–279.

BIA. 1963. Differential movement—Cause and effect—Part I. Brick Institute of America, Technical Notes on Brick Construction, No. 18.

BRE. 1979. Estimation of thermal and moisture movements and stresses: Part 2. Building Research Station, Garston, Watford, England, Building Research Establishment Digest No. 228.

CEB. 1976. Model code for concrete structures. Comité Européen du Béton, Bulletin d'Information No. 117-E, 3rd draft translation of the French master copy.

——— 1980. Manuel de calcul "Effets structuraux du fluage et des déformations différées." Comité Européen du Béton, Bulletin d'Information No. 136.

CSA. 1984*a*. Design of concrete structures for buildings. Canadian Standards Association, Rexdale, Ont., CAN3-A23.3-M84.

——— 1984*b*. Masonry design for buildings. Canadian Standards Association, Rexdale Ont., CAN3-S304-M84.

DAVISON, J. I. 1980. Linear expansion due to freezing and other properties of bricks. Second Canadian Masonry Symposium Proceedings, Ottawa, pp. 13–24.

ESKENAZI, A., OJINAGA, J., AND TURKSTRA, C. J. 1975. Some mechanical properties of brick and block masonry—interim report. McGill University, Montreal, P.Q., Structural Masonry Series No. 75-1.

FENTON, G. A. 1984. Differential movements and stresses arising in masonry veneers of highrise structures. M.Eng. Thesis, Department of Civil Engineering, Carleton University, Ottawa, Ont.

FENTON, G. A., AND SUTER, G. T. 1985. Differential movement between clay brick veneer and concrete block in loadbearing masonry highrise structures. Seventh International Brick Masonry Conference, Melbourne, Australia.

FINTEL, M., AND KHAN, F. R. 1969. Effects of column creep and shrinkage in tall structures—Prediction of inelastic column shortening. Journal of the American Concrete Institute, **66**, pp. 957–967.

GRIMM, C. T. 1981. Dimensional stability of clay masonry. Internal report, Center for Building Research, The University of Texas at Austin, Austin, TX.

HHFA. 1954. Shrinkage characteristics of concrete masonry walls. Housing and Home Finance Agency, Washington, DC, Paper No. 34.

JESSOP, E. L., BAKER, L. R., AMENY, P., AND KHALIL, K. R. 1978. Moisture, thermal, elastic, and creep properties of masonry. Department of Civil Engineering, University of Calgary, Calgary, Alta., Research Report No. CE78-16.

LENCZNER, D. 1970. Creep in brickwork. Proceedings of the Second International Brick Masonry Conference, British Ceramic Research Association, England.

——— 1980. Design of brick masonry for elastic and creep movements. Second Canadian Masonry Symposium Proceedings, Ottawa, pp. 303–316.

LOUBSER, P. J., AND BRYDEN, J. G. 1972. An apparatus for determining the coefficient of thermal expansion of rocks, mortars, and concretes. Magazine of Concrete Research, **24**(79), pp. 97–100.

MCDOWALL, I. C., AND BIRTWISTLE, R. 1970. Predicting the long term moisture expansion of fired clay products. Proceedings of the Second International Brick Masonry Conference, British Ceramic Research Association, England.

MONK, C. B. 1978. Analysis of nonstructural volume changes in masonry construction. Fifth International Brick Masonry Conference, Brick Institute of America, pp. 439–443.

NCMA. 1961. Concrete masonry shrinkage. National Concrete Masonry Association, Arlington, VI.

——— 1973. Design of concrete masonry for crack control. National Concrete Masonry Association, Arlington, VI, Technical Publication No. 53.

——— 1977. Strength and time-dependent deformations of reinforced concrete masonry. National Concrete Masonry Association, Arlington, VI, Technical Publication No. 84.

PALMER, L. A. 1931. Volume changes in brick masonry materials. Journal of Research of the National Bureau of Standards, **6**, pp. 1003–1026.

PLUMMER, H. C. 1962. Brick and tile engineering. 2nd ed. Structural Clay Products Institute, Washington, DC.

POLJAKOV, S. V. 1962. Some problems of creep in ordinary and reinforced masonry members. International Council for Building Research, Studies and Documentation, Paris.

ROSS, C. W. 1941. Thermal expansion of clay building bricks. Journal of Research of the National Bureau of Standards, **27**, pp. 197–216.

SCHUBERT, P. 1980. Control of the expansion and contraction behaviour of masonry bricks to avoid cracking damage. Ziegelindustrie International, No. 10, pp. 645–650.

SHEEHAN, P. K. 1976. Measurement of linear expansion. Experimental Building Station, Australia, Technical Record TR44/153/432.

STETINA, H. J. 1965. Structural steel construction. Building construction handbook, McGraw-Hill Book Company, New York, NY.

STURGEON, G. R. 1978. Deformations of concrete block and concrete block masonry. Civil Engineering Department, Carleton University, Ottawa, Ont., report for G. T. Suter.

STURGEON, G. R., LONGWORTH, J., AND WARWARUK, J. 1980. An investigation of reinforced concrete block masonry columns. Department of Civil Engineering, University of Alberta, Edmonton, Alta., Structural Engineering Report No. 91.

SUTER, G. T., AND HALL, J. S. 1976. How safe are our cladding connections? Proceedings of the First Canadian Masonry Symposium, Calgary, pp. 95–109.

WARREN, D., AND LENCZNER, D. 1981. A creep-time function for single-leaf brickwork walls. International Journal of Masonry Construction, **2**(1), pp. 13–20.

Appendix A. List of symbols

A_b a constant dependent on brick type for Poljakov's creep function

D_m maximum mortar moisture travel distance (mm) = $0.5d_w$ generally

d_m effective column or block-wall dimension (mm)

d_w wall thickness (mm)

E_{bl} modulus of elasticity of fully, partially, or ungrouted concrete block masonry (MPa)

E_c modulus of elasticity of concrete (MPa)

E_{gr} modulus of elasticity of grout as determined from standard moist cured cylinders (MPa)

E_m modulus of elasticity of clay brick masonry (MPa)

E_{ug} modulus of elasticity of ungrouted concrete block masonry (MPa)

f_a age-at-loading correction factor for creep of clay brick masonry

f'_{bl} ultimate concrete block unit compressive strength, based on net area (MPa)

f'_{br} compressive strength of brick unit (MPa)

f'_c specified compressive strength of concrete (MPa)

f'_{cm} 28-day mean compressive strength of concrete based on cylinder tests (MPa)

f'_m compressive strength of masonry (MPa)

f'_{mort} compressive strength of mortar (MPa)

h height of the supported masonry panel (mm)

K_c ratio of the volume of iron oxide to the original volume of iron (ranges from 1.4 to 4.1 with a mean value of 2.1)

k_j creep recovery correction factor
= 1.0 if $(\sigma_j - \sigma_{j-1}) \leq 0$ (i.e. compression force increasing)
= 0.67 if $(\sigma_j - \sigma_{j-1}) > 0$ (i.e. compression force decreasing)

R_{bl} ratio of the modular to nominal vertical concrete block dimensions

R_{br} ratio of modular to nominal vertical brick dimensions

RH mean relative humidity of the environment (%)

S_1 unadjusted ultimate shrinkage strain of concrete

S_2 shrinkage strain correction factor for effective thickness of concrete

T_i mean temperature of element at the time of interest (°C)

T_p mean temperature of element at its time of placement (°C)

t_{bl} true age of the concrete block unit at the time of construction (days)

t_{eff} effective age of the concrete block masonry at the time of construction (days)

t_i age of the concrete or masonry at the time of interest (days)

t_j age of the concrete or masonry at the beginning of interval j (days)

t_ℓ age of the brick masonry at the time of loading (days)

t_0 age of the concrete, masonry, or masonry unit at earlier time of interest, i.e. when placed or when shelf angle installed (days)

t_{sa} time at which the thickness reduction of the shelf angle was measured (days)

t_{sp} time at which the shelf angle was placed (days)

t_t age of the clay brick unit at the time of the moisture expansion test (days)

α fraction of concrete block masonry cores grouted

α_{th} coefficient of thermal expansion (mm/(mm·°C))

β_s variation of shrinkage with time function

γ_c density of concrete (kg/m^3)

Δd_c shelf angle thickness reduction due to corrosion occurring between the times t_{sp} and t_{sa} (mm)

ϵ_{blsu} ultimate shrinkage strain of the concrete block unit

ϵ_{bm} unrestrained moisture expansion strain of clay brick unit

ϵ_{bmt} measured or tested moisture expansion strain of clay brick unit

ϵ_{co} effective strain in the veneer due to corrosion of the steel shelf angle

ϵ_{cr} total unrestrained creep strain in the concrete or masonry at the time of interest t_i (at the end of interval $i - 1$)

ϵ_m unrestrained moisture expansion strain of clay brick masonry

ϵ_{msu} ultimate shrinkage strain of the mortar (see Table 3)

ϵ_{sh} unrestrained shrinkage strain

ϵ_{shbl} unrestrained shrinkage strain of concrete block unit

ϵ_{shgr} unrestrained shrinkage strain of the grouted core

ϵ_{shmo} unrestrained shrinkage strain of the mortar at the time of interest t_i

ϵ_{th} unrestrained thermal strain

η interpolation factor

σ_j total stress applied to the concrete at the beginning of interval j in MPa (assumed to be constant through-

TABLE B.1. Linear coefficients of thermal expansion of concrete for different aggregate types (from Grimm 1981)

Aggregate type	Thermal coefficient (μm/(m·°C))
Quartz	11.9
Limestone	6.8
Basalt	8.6
Granite	9.5
Gravel	10.8
Sandstone	11.7
Lightweight	8.1

TABLE B.2. Coefficients of thermal expansion of block work according to the references indicated

Reference	Aggregate	Thermal coefficient (μm/(m·°C))
Jessop *et al.* (1978)		6–13
BRE (1979)	Normal weight	6–12
	Light weight	8–12
BIA (1963)	Dense	9.4
	Cinder	5.6
	Expanded shale	7.7
	Expanded slag	8.3
	Volcanic pumice	7.4

TABLE B.3. Coefficients of thermal expansion of clay brick masonry given in various references

	Thermal coefficient (μm/(m·°C))				
		Brick unit			
Reference	Brick masonry	Clay	Shale	Mortar	Direction
NCMA (1973)	6.5	—	—	—	?
Bergquist (1979)	6.0	—	—	—	Vert.
BRE (1979)	5–8	—	—	10–13	?
Anderson (1976)	7.0	—	—	—	?
Schubert (1980)	5.9	—	—	—	?
BIA (1963)	6.5	—	—	—	?
Plummer (1962)	6.5	—	—	—	Hor.
Sturgeon (1978)	—	—	—	6.3–9.2	?
Loubser and Bryden (1972)	—	—	—	12.7	?
Baker (1964)	—	5.4	5.4	—	?
Ross (1941)	—	4.1–12.4	4.7–6.8	—	?
Palmer (1931)	—	4.7–8.5	4.1–5.2	8.5	?
Sheehan (1976)	—	4.1–8.1	—	—	Both
Monk (1978)	—	5.4	5.4	—	?

NOTE: ? indicates direction is not given.

out the interval)—compression is negative

σ_{ult} average ultimate strength of the brick masonry (MPa)

$\Phi(t_i, t_j)$ creep function giving the specific creep at the time of interest t_i due to the stress increment applied at the beginning of interval j (mm/(mm·MPa))

ψ ratio of the net concrete block area to the gross block area

Appendix B. Coefficients of thermal expansion

Typical coefficients of thermal expansion for concrete and masonry are given in Tables B.1–B.3.

Appendix C. CEB creep function

The creep function $\Phi(t_i, t_j)$ is given by CEB (1980) to be

$$\Phi(t_i, t_j) = \frac{1}{E_c(28)}[\beta_a(t_j) + \psi_d \cdot \beta_d(t_i - t_j) + \psi_{f1} \cdot \psi_{f2}\{\beta_f(t_i) - \beta_f(t_j)\}] \quad [C.1]$$

where

$\beta_a(t_j)$ = plastic flow developed in the first day after load application

$$= 0.8 - 0.16948 \ln (1.1631 t_j) + 0.16785 \times \ln\left(1 + \frac{t_j}{93.09}\right) \quad [C.2]$$

ψ_d = coefficient for delayed elastic strain

$$= 0.4$$

$\beta_d(t_i - t_j)$ = delayed elastic strain function

$$= 0.17196 \ln [0.57236(t_i - t_j)] + 0.07541 \times \ln\left[1 + \left(\frac{16.5576}{t_i - t_j}\right)^{1.8}\right] - 0.08855 \times \ln\left[1 + \left(\frac{t_i - t_j}{637.71}\right)^2\right] \quad [C.3]$$

ψ_{f1} = relative humidity flow coefficient

$$= 4.1034\left(1 - \frac{RH}{100}\right)^{0.613} \quad [C.4]$$

TABLE C.1. Coefficients for use in [C.9] for the calculation of the delayed plastic flow in concrete

d_m	a	b	c	d	f	g	P	Q
50	0.16603	0.41521	0.06664	6.1055	0.10163	749.792	1.50	1.50
100	0.16036	0.40458	0.04326	9.8208	0.10755	1141.435	2.00	1.40
200	0.16026	0.31470	0.06444	11.5717	0.14694	1769.201	1.50	1.10
400	0.14482	0.23919	0.11935	13.1296	0.11154	5415.922	0.80	1.45
800	0.14913	0.11974	0.08257	86.8109	0.07507	7666.979	1.00	2.10
1600	0.19089	0.02592	0.07348	290.8034	0.11871	8979.504	1.80	1.80

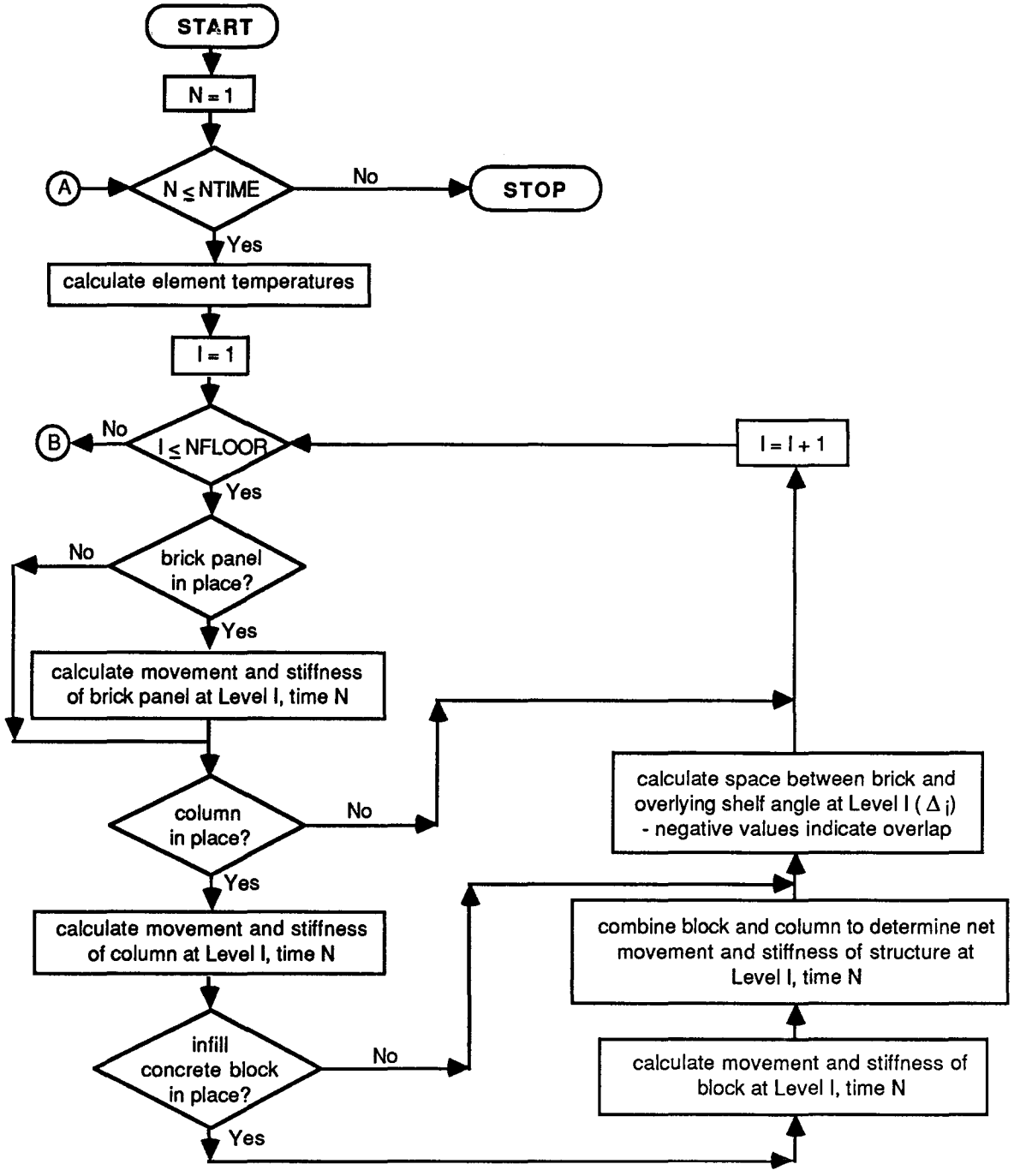

FIG. D.1. Flow chart of iterative procedure. Notation: ITER = iteration counter, MAX = maximum number of iterations, NFLOOR = number of levels in the structure, NTIME = number of time intervals considered in the analysis, POLD, PNEW = old (last iteration) and new (present iteration) axial forces acting in the veneer due to shelf angle shear forces, Δ_i = gap between shelf angle and underlying veneer (negative values indicate an overlap).

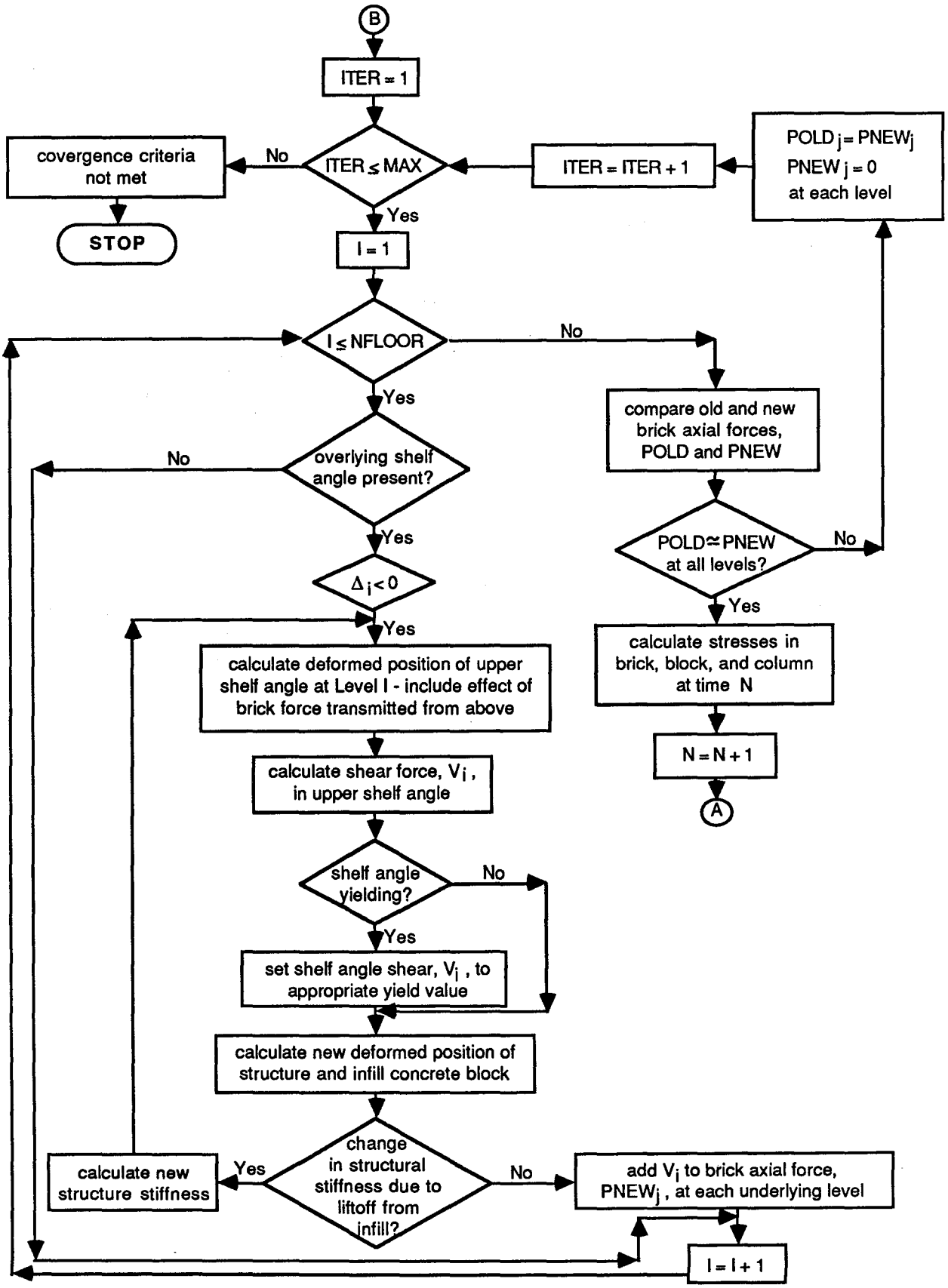

FIG. D.1. (*Concluded*).

RH = relative humidity of the environment in percent

ψ_{f2} = effective thickness flow coefficient

[C.5] $$= 5.67525\left(\frac{1}{d_m}\right)^{0.05} - 2.8045$$

d_m = effective thickness of the column or wall (mm)

[C.6] $$= \lambda\left(\frac{2A_c}{P}\right) \quad \text{for a column}$$

[C.7] $$= \lambda \cdot d_w \quad \text{for a concrete block masonry wall}$$

d_w = wall thickness (mm)

λ = ambient environment coefficient

[C.8] $$= 0.98 + 4.0478 \times 10^{-4} e^{0.10226(RH)}$$

A_c = cross-sectional area of the column (mm^2)

P = perimeter length of the column cross section (mm)

$\beta_f(t)$ = delayed plastic flow function

The delayed plastic flow function β_f is quite complex, varying both with time and the effective thickness d_m. The following relationship has been developed for the computer to allow a fairly precise evaluation of β_f:

[C.9] $$\beta_f(t) = a \ln (bt) + c \ln\left[1 + \left(\frac{d}{t}\right)^P\right] - f \ln\left[1 + \left(\frac{t}{g}\right)^Q\right]$$

where the coefficients a, b, c, d, f, g, P, and Q vary for different values of d_m as shown in Table C.1. To interpolate for intermediate values of d_m (for example d_m = 275 mm),

(1) Let d_1 be the next lower value of d_m for which an equation or curve exists (i.e. d_1 = 200 mm), and d_2 be the next higher (i.e. d_2 = 400 mm).

(2) Calculate $\beta_{f1}(t)$ for d_1 (i.e. for d_m = 200) and $\beta_{f2}(t)$ for d_2 (i.e. for d_m = 400).

(3) Calculate the interpolation factor η to be

[C.10] $$\eta = \left[\frac{d_m - d_1}{d_2 - d_1}\right]^{0.6} = \left[\frac{275 - 200}{400 - 200}\right]^{0.6}$$

(4) Calculate the desired $\beta_f(t)$ value as follows:

[C.11] $$\beta_f(t) = \beta_{f1}(t) - \eta[\beta_{f1}(t) - \beta_{f2}(t)]$$

Appendix D. Computer program

Figure D.1 is a flow chart of the iterative procedure used to estimate the structural forces arising from differential movement between the veneer and its support. A solution is obtained when the axial forces produced in the brick veneer on one iteration are acceptably close to those calculated in the previous iteration.

The flow chart is greatly condensed and somewhat simplified to make it manageable in this paper, representing, as it does, some 3000 lines of FORTRAN code. In particular the flow chart describes the procedure used for reinforced concrete or steel structures with shelf angles that are not able to deform downwards from their rest positions. The latter will occur, in general, when no movement joints are provided—that is, all underlying shelf angles are supported by the veneer.

A complete description of the program is given by Fenton (1984) and the program listing is available from G. T. Suter, Department of Civil Engineering, Carleton University, Ottawa, Ont., who should be contacted concerning the medium of transfer for this program.